

Demand Response for Natural Gas: Technologies, Mathematical Models, and Challenges Ahead

Fuyu Hu¹, Kaarthik Sundar^{2,*}, Shriram Srinivasan¹, Russell Bent¹

Abstract

Demand response in the context of electrical power networks is a mature field, but the study of its counterpart for natural gas networks is still in its infancy. This work is timely given the realities of climate change; according to some models, climate change will increase the number of severe winter weather events that will create stress on the natural gas pipeline networks, impeding the ability of these systems to provide equitable services to all its customers. The lack of resiliency in natural gas pipeline systems results in inconvenience, disruption and even loss of lives. This article addresses the important problem of demand response for residential natural gas consumers, namely, the reduction of nominal and peak gas demand during normal winter weather as well as severe winter weather events such as those induced by polar vortices. We systematically develop a mathematical model for demand response of thermal heating systems at a household level. The developed models are leveraged as physical constraints in formulating optimal control problems that optimize the gas consumption of a collection of houses, with goals being twofold – reduction of peak gas demand along with equitable service. On our test problems, we demonstrate significant benefits, including the ability to cut peak demand by 15% while still ensuring equitable service to customers. We discuss the limitations of current technology and the advancements that are needed to implement such demand response programs in practice. Furthermore, we also enumerate the research challenges and open problems that need to be solved to make such demand response programs viable for natural gas systems in the near future.

Keywords: natural gas demand response, smart thermostats, optimal control, polar vortex, mixed-integer optimal control

1. Introduction

In energy systems, demand response (DR) is an option offered to energy consumers by system suppliers and operators for shifting energy usage away from peak consumption periods. DR programs are typically voluntary and operators use time-based rates or economic incentives to encourage participation. Within

*Corresponding author

Email addresses: fuyuhu@lanl.gov (Fuyu Hu), kaarthik@lanl.gov (Kaarthik Sundar), shrirams@lanl.gov (Shriram Srinivasan), rbent@lanl.gov (Russell Bent)

¹Applied Mathematics and Plasma Physics Group, Los Alamos National Laboratory.

²Information Systems and Modeling Group, Los Alamos National Laboratory.

the electric power industry (the largest adopter of DR technologies), there are numerous studies that have demonstrated the benefits of DR programs. For example, in the United States, the Federal Energy Regulatory Commission (FERC) announced a national DR action plan in 2009 for maximizing the adoption of DR through the execution of a national communication program, the development of analytical tools, the outlining of regulations, and examples of model contracts [1]. FERC's national assessment of DR potential predicted that by 2019 peak load could be reduced by as much 150 GW (the output of roughly 2000 power plants) should DR be adopted nationwide [2]. Subsequent reports have estimated that actual adoption of DR saved approximately 2,133 MW in wholesale markets (2018) and approximately 30,000 MW in retail markets (2017).

While the primary motivation for wide-scale adoption of DR is reduction in peak consumption, there are auxiliary benefits. For example, overall reduction in peak consumption improves utilization of existing capacity and delays or eliminates the need for costly capacity expansions. Since many electric power plants run on natural gas, cutting down peak consumption reduces the amount of natural gas undergoing combustion and thus, demand response technologies can also reduce greenhouse gas emissions [3]. In a recent study, the Electrical Power Research Institute (EPRI) predicted that DR could reduce the existing carbon emissions by 60 to 210 million metric tons within 2030 [4]. Finally, DR is also a tool for improving reliability and reducing operational risk. For example, PJM (the operator of the largest electric grid system in North America) has used DR to pro-actively curtail demand at commercial and industrial facilities prior to an exceptionally strong heat wave [5].

Electric power DR generally relies on two technologies: load control devices and market strategies. Market strategies are used to price electric power in different ways so as to provide incentive for the consumption of power at times desirable to the system operator [6]. On the other hand, load control devices (energy storage, power-heating switch devices, etc.), are used to directly flatten the energy demand by moving consumption from times with high utilization to times with low utilization. One example of load control that is widely used in electric power DR programs is home cooling systems during summer months. Here, thermal inertia is used to pre-cool buildings prior to peak demand hours.

Optimization is the core computational technology used for investigating and controlling DR. Within the literature, both deterministic and stochastic optimization methods have been developed. Deterministic models assume that all information is known by the users and the operators [7, 8]. Stochastic models introduce uncertainty associated with supply, demand, price, customer behavior, environmental variables, etc. [9, 10, 11, 12, 13, 14, 15, 16]. The objective functions consider factors like economic benefits due to energy cost savings [17, 18], operation profits [15, 19, 20, 21]), engineering needs such as reliability [22], risk minimization [15], greenhouse gas emission reductions [23, 16], or social welfare in the form of customer costs [19, 14] and user comfort [24]). One other line of work on optimal control of an ensemble of Thermostatically Controlled Loads (TCLs) [25, 26, 27] is very closely related to the models and DR formulations that are presented in this article for a natural-gas only setting. Optimal control problems for an ensemble of

TCLs reduce the electricity consumption from TCLs (typically air-conditioners) during the summer months by utilizing thermal inertia to its advantage. In this line of work [25], a simple Newtonian thermal model (an RC circuit model) for heat exchange between the surroundings and a house is utilized to change consumption patterns with the objective of reducing the price the consumer pays for electricity. We use similar thermal models in this article to develop a DR program in a natural-gas only setting to cater to the heating needs of the households in winter months.

While DR response has been a part of the electric power industry's technology adoption conversations for at least a decade, it is only recently that such technologies have been discussed in the context of other energy industries. Within the natural gas industry, DR technologies are discussed in two contexts. Firstly, historically low prices in natural gas have greatly expanded its utilization and placed an enormous strain on existing capacity [28]. At the same time, economic, political, and social factors have limited the ability of the industry to add capacity [29]. As a result, DR has been proposed as a technology for improving the utilization of existing capacity [30]. Secondly, extreme events like the polar vortices and the recent cold snap in Texas have created relatively sudden spikes in the natural gas consumption for home and commercial heating leading to loss of load to millions of homes. Such events have the potential to create supply and capacity shortages that interrupt gas deliveries. During recent events, states like Minnesota have employed extreme measures like asking customers to decrease thermostat set-point temperatures to 60 F to counter such demand spikes [31]. Despite the potential for DR to support the natural gas industry in both these contexts, work and approaches for modeling and controlling demand response in natural gas systems has been limited (unlike electric power).

There has been limited research on natural gas as a supplemental energy resource for electric power DR. Cui et al. [20] developed a demand response market model where natural gas based generation provides a supportive role for electric power demand response. Later, Qadrdan et al. [18] developed a model of the combined electric and natural gas system in Great Britain and used it to study the influence of DR in combined system modeling. Su et al. [16] use electric power demand response technologies like pumped storage and incentives to improve the operational performance of coupled natural gas and electric systems. Finally, Zhang et al. [32] developed a pricing strategy to maximize the social benefits of demand response in coupled gas-grid systems. In all these papers, the focus was largely on how DR in power systems could impact the operations of joint gas-electric systems.

Even though natural gas is an important energy resource in isolation [33], only a few papers have considered demand response in natural gas systems. For example, Abahussain and Christie [34] described a price-based demand response for optimal scheduling of deferrable gas loads (power plants) to maximize profits. Rudkevich and Zlotnik [35] developed a combined pricing mechanism to schedule production and consumption of natural gas systems to maximize social welfare. In both cases, the papers focused on large industrial loads with deferrable consumption patterns. Another motivating factor to design a gas-only DR programs arises due to the seasonality of natural gas consumption patterns. During the summer months

the major consumers of natural gas are the industrial gas-fired power plants that produce electricity by burning natural gas. The electric DR programs that are widely used indirectly reduce the amount of natural gas consumption from these industrial customers during these months. On the other hand, during the winter months, apart from industrial consumption of natural gas (gas-fired generators) to generate electric power, home heating systems become a major source of gas consumption. In this scenario, the gain in capacity and flexibility provided to the natural gas system by the electric DR programs is not sufficient to cater to all the consumers' natural gas needs. These issues are compounded during extreme weather events like the polar vortex in 2019 and the recent cold weather snap in Texas in 2021 where the natural gas infrastructure becomes extremely stressed. Hence, a natural gas-only DR program focused on residential home heating needs would alleviate the stress in the natural gas system to some extent. We envision these natural gas-only DR programs, when implemented in conjunction with the already available electric DR programs, would provide the necessary flexibility to deliver natural gas to both industrial and residential consumers in a reliable manner.

To address these issues, we develop a model of natural gas demand response at the household level based on physics and thermodynamics motivated by the recent work on optimal control formulations for controlling an ensemble of TCLs [25]. Here, we focus on smaller consumers, who are a significant source of DR capability in electric power systems but are yet to be studied in natural gas systems. Since home heating systems are the major source of natural gas consumption in residential households, the model proposed in this paper optimizes the gas consumption (home heating) of a collection of houses to reduce peak gas demand during normal winter operation as well as during extreme temperature events such as those induced by severe weather events. For the purposes of this paper, we focus on developing a deterministic natural gas demand response model to identify and study consumption patterns and peak reduction opportunities to analyze targets that can be achieved without too much reduction in performance of home heating systems.

The DR problem is formulated as an optimal control problem (OCP) in multiple ways. In each case, it is a mixed-integer optimization problem coupled with ordinary differential equations that model the dynamics of house temperature (heat gain from gas-fired furnaces and heat loss to the surroundings due to cooler external temperatures). The OCPs differ from each other in either of the following two aspects: (i) implementation of the control policy (centralized or decentralized) and (ii) objective of the OCP which can either be to keep household temperatures as close to a desired set point as possible while keeping peak consumption below a specified threshold, or to reduce the overall gas consumption while keeping temperature deviations to a pre-specified limit or a combination of both. Overall, the goal of all the OCPs presented in this article is to assess (qualitatively and quantitatively) the merits of a DR policy through the viewpoint of both the natural gas system operator and the residential customers. The models are also serve as an important first step towards identifying requirements for DR technologies and market structures. In summary, the key contributions of this paper include

- A simple Ordinary Differential Equation (ODE) model inspired by dynamic models for TCLs for a home heating system that is leveraged to formulate OCPs that optimize natural gas load scheduling at a household level.
- A receding-horizon based algorithm to solve the resulting OCPs after discretization.
- Empirical studies which highlight the aggregation benefits and the degree of thermostat flexibility required to achieve a certain level of peak reduction.
- A detailed discussion of the open research challenges that lie ahead in the task to bring DR for natural gas systems into practice.

The remainder of this paper is organized as follows: Section 2 discusses a high level description of the problem while In, Section 3, we present a baseline model to reflect current practice and formulate the physics-based, decentralized and centralized natural gas demand response models and describe the solution method in Section 4. Finally, Section 5 presents the case studies and simulation results and Section 6 concludes the paper and offers future perspectives.

2. Problem setup and assumptions

Figure 1 shows a conceptual diagram of a consumer level demand response program in natural gas systems proposed in this article. In this scenario, the operator of the natural gas system seeks to reduce natural gas consumption during normal operation in the winter months and also in response to an extreme temperature event like a polar vortex. To that end, households sign up for a demand response program designed by the operator to meet the reliability goals and customer satisfaction needs . Given the practical challenges associated with direct participation in the demand response programs, we adopt a load aggregator model (blue boxes in Fig. 1) often used in the electric power DR program. Load aggregators recruit participants for the DR program, interact with the markets, and coordinate response to meet the operator consumption requirements.

The aggregators face three key technical challenges:

1. Satisfying the consumption requirements and ensuring customer satisfaction.
2. Providing socially equitable services to the DR participants.
3. Identifying parameters for pricing incentives for participation.

A key component of load aggregation is ensuring relatively equal distribution of adverse conditions to participants. In this context, adverse condition is thermal discomfort (modelled as average deviation or the maximum deviation from temperature set points) which has detrimental effects on human health and performance [36, 37, 38]. The requirement of equitable distribution and customer satisfaction is enforced by optimizing a social welfare objective function which indirectly minimizes the thermal discomfort. The final

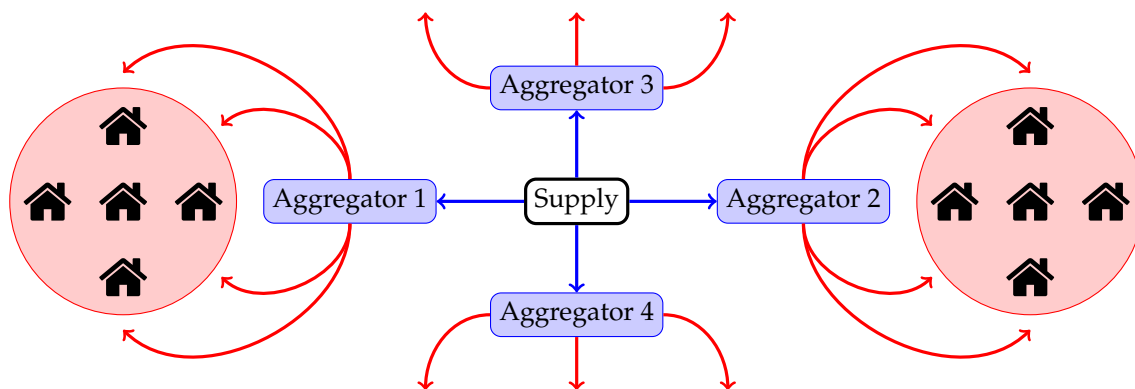


Figure 1: Conceptual diagram of a natural gas DR system. The aggregator implements the DR program for the set of houses that it caters to. Here, aggregator may refer to a natural gas utility company in a particular geographic location.

challenge for the aggregator is participant incentives. The participants need incentives (typically monetary) to give up temperature comfort in their homes. While it is outside the scope of this paper to develop an incentive program, this paper does identify key parameters (maximum temperature deviation and number of participants) needed for choosing incentive levels.

The DR problem is an optimal control problem and while we have already alluded to the objective or cost function which needs to be optimized, there also exist constraints consisting of the governing equations describing the dynamics and control of the system. We mentioned earlier that DR in the context of electric power networks is well developed, while DR in the context of natural gas systems is in its infancy. Thus, there arises a natural tendency to transfer the methods and approaches successful in DR of electric power networks into the context of natural gas systems. To that end, in this article, we utilize thermodynamic models of heat flow that are used in the context of TCLs [25, 27] and build natural-gas only DR formulations on top of these dynamic models.

In the subsequent sections, we develop a model of natural gas demand response at the household level with an overarching goal of helping the natural gas utility operator or aggregator to quantitatively measure the efficacy of a natural gas DR program in the locality. We make the following strong assumptions that will serve two purposes: (i) they will aid in simplifying the mathematical model to a great extent and (ii) the solutions provided in this simplistic setting will provide a worst-case guarantee on the benefits of using DR programs for a natural gas-only setting. The assumptions are:

1. The natural gas utility operator aggregates the natural gas demand or load from all the households in the locality. Hence, from here on, we will use the term natural gas utility operator and aggregator interchangeably.
2. The only source of natural gas consumption for the households is home heating. This is justified because the home heating systems are the major source of natural gas consumption in most households during the winter months. In summer months, the major sources of natural gas consumption are in-

dustrial loads and gas-fired power plants; however, these type of loads are not the primary focus of this article.

3. Each participating household in the DR program has a smart thermostat installed; in this article, we consider two kinds of smart thermostats (“Type 1” and “Type 2”) with different capabilities. The “Type 1” thermostat is capable of (a) obtaining a temperature forecast for the future, (b) allowing the customer to establish a temperature set-point of the thermostat, (c) allowing the customer to choose a parameter that adjusts the priority of the thermostat between maintaining a set-point temperature to saving on gas consumption and finally, (d) has minimal computing capability to solve optimization problems. The use of a “Type 1” thermostat permits a decentralized control policy as no information is shared between households or between the household and the aggregator. The “Type 2” thermostat is capable of (a) sending the current temperature of the house and the set-point temperature of the thermostat to the aggregator and (b) receiving on-off control policy from the aggregator that it implements. This is a strong assumption and it inherently makes the control policy that uses this smart thermostat a centralized one. Unlike the “Type 1” thermostat, the “Type 2” thermostat does not perform any computation and all of the computation is offloaded to the aggregator.
4. Effects of the actual distribution pipeline network used to deliver gas to the households are ignored.

Parts of the third and the fourth assumptions are strong. However, this is a viability study, and we argue that if one does not quantitatively or qualitatively find any benefit to using the DR model despite these assumptions, any other DR formulation in a natural gas-only setting with more practical assumptions will only do worse and be unviable. In the next section, we present a few notations and the different DR optimal control problem formulations.

3. DR optimal control problems

Before we present the different Optimal Control Problem (OCP) formulations for the DR problem in a natural gas-only setting, we introduce some notations. In a locality where a DR program is implemented, we denote by \mathcal{H} the set of houses, and index each house by h . We let $\theta^o(t)$ be the given time-varying forecast of the ambient/outside temperature. We also let θ_h^0 denote the initial temperature inside house h . Each house is assumed to have a gas furnace that burns fuel at the rate Q (kg s^{-1}). For each house $h \in \mathcal{H}$, we let $\{\alpha_h, \beta_h\}$ denote its thermal coefficients. Also associated with each house h are the following state and control variables: $\theta_h(t)$ - current temperature of the house (K), $q_h(t) \in \{0, 1\}$ - a binary control variable that controls supply of natural gas. Finally, we let $d_h(t)$ denote the time-varying natural gas consumption of the house h . For each household $h \in \mathcal{H}$, we denote the DAEs that govern the thermodynamics of heating

by the following equations:

$$\dot{\theta}_h(t) = -\alpha_h \cdot (\theta_h(t) - \theta^o(t)) + \beta_h \cdot Q \cdot q_h(t) \quad \forall t > 0, \quad (1a)$$

$$\theta_h(t = 0) = \theta_h^0, \text{ and} \quad (1b)$$

$$q_h(t) \in \{0, 1\}. \quad \forall t \quad (1c)$$

The Eq. (1a) is a simple Newtonian equation that captures the dynamics of heat flow within the house h . A similar equation has been used previously to model TCLs in the electric power literature [25]. In Eq. (1a), $\dot{\theta}_h(t)$ is used to indicate the time derivative of the temperature of the house. The algorithm to compute the thermal coefficients $\{\alpha_h, \beta_h\}$ for each house $h \in \mathcal{H}$ is provided in Appendix A. The Eq. (1b) – (1c) define the initial conditions for $\theta_h(t)$ and the binary restrictions on the on-off control variable $q_h(t)$, respectively. Utilizing the above dynamic equations, we now present a baseline model that is reflective of current practice for households in the US.

3.1. Baseline model

In the baseline model, each house is equipped with a normal thermostat that is available in the market. By normal thermostats, we mean that the thermostat implements an instantaneous control policy, i.e., at any time instant t , it decides to turn-on or turn-off the gas supply if the current temperature of the house is less or greater than (respectively) the set-point temperature of the thermostat. This is reflective of the thermostats that are currently deployed in majority of the households in the United States. For this baseline model, the control policy is defined by the following equation

$$q_h(t) = H\left(1 - \frac{\theta_h(t)}{\bar{\theta}_h}\right) \quad \forall t > 0 \quad (2)$$

In Eq. (2), $H(\cdot)$ is the Heaviside step function and $\bar{\theta}_h$ is the set-point temperature of the thermostat. The above model is a decentralized model since implementing the control policy in each household $h \in \mathcal{H}$ requires only local information from h . The baseline model is integrated over a finite time horizon $[0, T]$ to obtain a solution $\theta_h^*(t)$ and $q_h^*(t)$ for every $h \in \mathcal{H}$. The mass flow rate of natural gas consumed by all the houses in the set \mathcal{H} can then be computed from the solution as:

$$d^b(t) = \sum_{h \in \mathcal{H}} Q \cdot q_h^*(t) \quad (3)$$

In Eq. (3), d^b represents the total mass flow rate of gas consumed (in kg s^{-1}) by all the houses in the set \mathcal{H} towards their home heating needs in winter. We refer to this value as the baseline gas consumption for a set of households in \mathcal{H} . In the next section, we present changes to the baseline model with the introduction of a smart thermostat with certain capabilities.

3.2. Decentralized look-ahead model

To formulate the decentralized look-ahead model, we assume that each house $h \in \mathcal{H}$ is equipped with a “Type 1” smart thermostat. The output of this model is a decentralized on-off control policy for each

house h ; this policy is decentralized in the sense that the control policy for each household is dependent only on current temperature and the parameters that are set in the thermostat in that house. This model is termed as a look-ahead model because, unlike the baseline model that does not take into account a forecast of the ambient temperature, this model accounts for this forecast and computes a control policy accordingly. Given these assumptions, we introduce additional notations to formulate this decentralized look-ahead optimal control formulation. As mentioned in the previous section, the Type 1 thermostat has the capability to obtain a temperature forecast, $\theta^0(t)$, up to a set time T in the future (referred to as the optimization time horizon). The first parameter that is set in the thermostat is the desired temperature set-point, $\bar{\theta}_h$ that the user wants to maintain inside the house $h \in \mathcal{H}$ and the second parameter $\lambda_h \in [0, 1]$ represents the mode in which the thermostat operates. When the value of $\lambda_h = 1$, the thermostat keeps the maximum deviation of the house temperature from its set point to a minimum for the entire optimization time horizon, i.e., the DR OCP seeks to compute a control policy that minimizes the maximum deviation over the entire time horizon, defined by $\Delta_h \triangleq \max_{t \in (0, T]} |\bar{\theta}_h - \theta_h(t)|$. On the other hand, when $\lambda_h = 1$, the thermostat computes a control policy that minimizes the total natural gas consumption over the entire optimization time horizon (see Eq. (4c)). For all other values of $\lambda_h \in (0, 1)$, the objective is to minimize a convex combination of Δ_h and G_h with λ_h as the multiplier; this in turn represents a trade-off between these outcomes. However, this trade-off cannot be quantified *a priori*, in the sense that it is not possible to choose a value of λ_h that will guarantee a certain outcome for either Δ_h or G_h unless we solve for the pareto front. Since that is a complexity best avoided at this stage, for a given problem the optimization will have to be performed for various values of λ_h and after an examination of the resultant values of Δ_h and G_h , a suitable value of λ_h can be chosen. Given the advancements in smart devices, a Type 1 thermostat can easily be engineered and deployed in large scales for many households within the country to implement such a decentralized look-ahead model. With the aforementioned assumptions and set-up, the OCP formulation of the decentralized look-ahead model that the smart thermostat solves for each house $h \in \mathcal{H}$ is as follows:

$$\min : \lambda_h \cdot \Delta_h + (1 - \lambda_h) \cdot G_h \quad (4a)$$

$$\text{subject to: } \dot{\theta}_h(t) = -\alpha_h \cdot (\theta_h(t) - \theta^0(t)) + \beta_h \cdot \mathbf{Q} \cdot q_h(t) \quad \forall t \in (0, T], \quad (4b)$$

$$G_h = \mathbf{Q} \cdot \int_0^T q_h(t), \quad (4c)$$

$$\theta_h(t = 0) = \theta_h^0, \quad (4d)$$

$$q_h(t) \in \{0, 1\}, \quad \forall t \in (0, T] \quad (4e)$$

$$\bar{\theta}_h - \Delta_h \leq \theta_h(t) \leq \bar{\theta}_h + \Delta_h \quad \forall t \in (0, T]. \quad (4f)$$

Here, the optimal control policy for each house can be obtained by solving the OCP in (4) corresponding to that house and this requires only local information. In the next section, we present two centralized look-ahead OCP models that allow the operator to have more fine-grained control of the consumption patterns of the household.

3.3. Centralized look-ahead models

The question motivating the centralized look-ahead models presented in this section is – if the aggregator knows daily consumption patterns for the group of houses that are participating in the DR program and the historical forecast, can the aggregator compute centralized control policies to achieve peak shaving during an extreme event like polar vortex while at the same time providing equitable services to all the customers? To that end, we start by assuming that all the households that participate in this DR program are equipped with a Type 2 thermostat that is capable of two-way communication with the aggregator. Unlike a Type 1 thermostat, the Type 2 thermostat has no computational capability, can send the temperature set-point and the current temperature of the house to the aggregator, and can receive and implement an on-off control policy computed by the aggregator. The look-ahead feature of these models arises from the fact that the aggregator has a forecast of the ambient temperature for the duration of the optimization time horizon and uses it to compute the control policy. The model is said to be a centralized one due to the fact that the aggregator utilizes (i) set-point temperature of each household, (ii) initial temperature of each household, (iii) parameters of each house, (iv) ambient temperature forecast, and (iv) additional constraints on consumption to solve a single OCP and compute a control policy for each household. The computed control policy is then transmitted to the thermostat in each household for implementation.

Technologically, implementing such a centralized DR model would involve massive investment in the infrastructure to set up two-way communication capabilities between the aggregator and the households. In this regard, the current internet or cellular backbone infrastructure can also be reused to achieve this communication capability. Furthermore, the use of such an architecture would entail resolving privacy and security concerns that arise due to communicating house data to an aggregator or a centralized authority. Nevertheless, we present these models with the goal of examining if there is any benefit to using a centralized DR model with the argument that this idealized model provides an upper bound to the benefits that will not be exceeded by any other DR model with more realistic assumptions. To that end, we develop and formulate two centralized look-ahead models, with the difference being in the objective functions used for the respective models. Similar to the decentralized look-ahead models, we assume that the optimization time horizon is $[0, T]$. We again let Δ_h denote the maximum deviation between the set-point temperature and the actual temperature of house h over the entire optimization time horizon. Also, to model peak shaving, we let D denote the maximum total amount of gas consumed by all the households in \mathcal{H} and let $\gamma \in (0, 1]$ denote the percentage of gas reduction that the aggregator achieves with the centralized DR program. With these notations, we present the following two centralized look-ahead models with two different objective functions (i) mean deviation objective and (ii) max deviation objective:

$$\text{Mean Deviation: } \min \frac{1}{|\mathcal{H}|} \sum_{h \in \mathcal{H}} \Delta_h \quad (5a)$$

$$\text{Max. Deviation: } \min \left(\max_{h \in \mathcal{H}} \Delta_h \right) \quad (5b)$$

In both the objective functions, the value of Δ_h for each house can be interpreted to denote the discomfort of the occupants. Then, the objective function in Eq. (5a) and Eq. (5b) minimizes the average and maximum discomfort, respectively, over all the households participating in the DR program. The centralized look-ahead OCP model with either of the objective functions in Eq. (5) is subject to the following constraints:

$$\dot{\theta}_h(t) = -\alpha_h \cdot (\theta_h(t) - \theta^o(t)) + \beta_h \cdot \mathbf{Q} \cdot q_h(t) \quad \forall t \in (0, T], \forall h \in \mathcal{H}, \quad (6a)$$

$$\theta_h(t=0) = \theta_h^0, \quad \forall h \in \mathcal{H} \quad (6b)$$

$$q_h(t) \in \{0, 1\}, \quad \forall t \in (0, T], \forall h \in \mathcal{H} \quad (6c)$$

$$\bar{\theta}_h - \Delta_h \leq \theta_h(t) \leq \bar{\theta}_h + \Delta_h \quad \forall t \in (0, T], \forall h \in \mathcal{H}, \quad (6d)$$

$$\sum_{h \in \mathcal{H}} \mathbf{Q} \cdot q_h(t) \leq \gamma \cdot \mathbf{D} \quad \forall t \in (0, T]. \quad (6e)$$

The constraint in Eq. (6e) enables the operator to enforce a peak mass flow rate of $\gamma \cdot \mathbf{D}$. Here, γ and \mathbf{D} are assumed to be known a priori; usually the system operator has a reasonable estimate of how much total gas is consumed by all the households during winter peaks and γ is a percentage factor that the operator can vary to perform reliability analysis in the case of an extreme event scenario. In this article, we refer to γ as the curtailment factor that indicates the percentage by which the operator wishes to curtail the maximum mass flow rate in the natural gas system. Thus, the centralized model offers an advantage over the decentralized one in that once γ is chosen, the operator already knows what to expect regarding peak consumption, and if the deviation performance corresponding to a chosen value of γ is unsatisfactory, then it is clear that a lower value of γ needs to be considered to achieve better deviation performance. Of course, such a constraint (Eq. (6e)) is pertinent only when considered from the viewpoint of the aggregator who deals with the total demand of the ensemble of houses, and is hence not meaningful in the context of a decentralized model.

The Fig. 2 presents a summary of the different models presented thus far in terms of the computation cost incurred for large-scale implementation and technological/infrastructure investment required to bring the corresponding DR program to practice.

The reader would have doubtless noticed that neither formulation, decentralized or centralized, make explicit the role of the optimization time horizon T . This will be made apparent in the subsequent sections when we present algorithmic approaches to solve the OCPs.

4. Algorithms

In this section, we present a receding-horizon algorithm to solve the decentralized and centralized look-ahead models. To solve these models, we first resort to time discretization of the state and control variables. We present all the algorithms utilizing a single fine discretization for both the state and the control variables. The choice of a very fine discretization for the control variables can lead to chattering [39] and this issue

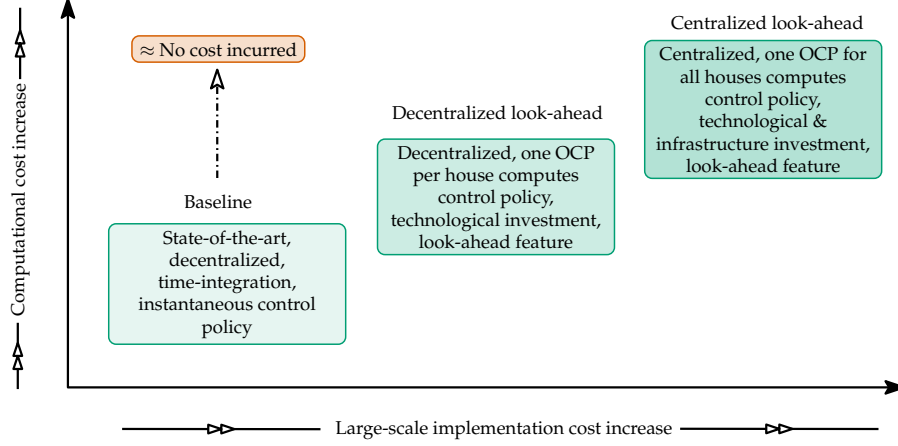


Figure 2: A summary of all the proposed OCPs for DR in a natural-gas only setting

can be avoided by utilizing a coarser time-discretization for the control variables. Nevertheless, for ease of exposition, we do not do so in the presentation of the algorithms. Before we present the receding-horizon algorithm, we first present a discretized version of the decentralized and centralized look-ahead models.

If we assume the optimization time horizon $[0, T]$ is discretized into n equispaced time instants $\mathcal{K} = \{0 = t_0, t_1 = \Delta t, \dots, t_n = n\Delta t = T\}$ with a time step of $\Delta t = T/n$, for every house $h \in \mathcal{H}$, the decentralized look-ahead model after discretization results in a Mixed-Integer Linear Program (MILP) as follows:

$$\min : \lambda_h \cdot \Delta_h + (1 - \lambda_h) \cdot G_h \quad \text{subject to:} \quad (7a)$$

$$\frac{\theta_h(t_{k+1}) - \theta_h(t_k)}{\Delta t} = -\alpha_h(\theta_h(t_k) - \theta^o(t_k)) + \beta_h \cdot \mathbf{Q} \cdot q_h(t_k), \quad \forall k \in \{0, \dots, n-1\} \quad (7b)$$

$$\theta_h(t_0) = \theta_h^0, \quad (7c)$$

$$G_h = \mathbf{Q} \cdot \sum_{k=0}^n q_h(t_k), \quad (7d)$$

$$\bar{\theta}_h - \Delta_h \leq \theta_h(t_k) \leq \bar{\theta}_h + \Delta_h \quad \forall k \in \mathcal{K}, \quad (7e)$$

$$q_h(t_k) \in \{0, 1\} \quad \forall k \in \mathcal{K} \quad (7f)$$

As for the MILPs for the centralized models, they have to be solved as a single optimization problem for all houses due to the inherent centrality in the decision making process. The constraints of these MILPs after discretization, are as follows:

$$\frac{\theta_h(t_{k+1}) - \theta_h(t_k)}{\Delta t} = -\alpha_h(\theta_h(t_k) - \theta^o(t_k)) + \beta_h \cdot \mathbf{Q} \cdot q_h(t_k), \quad \forall k \in \{0, \dots, n-1\} \quad (8a)$$

$$\theta_h(t_0) = \theta_h^0, \quad \forall h \in \mathcal{H} \quad (8b)$$

$$\bar{\theta}_h - \Delta_h \leq \theta_h(t_k) \leq \bar{\theta}_h + \Delta_h \quad \forall k \in \mathcal{K}, h \in \mathcal{H}, \quad (8c)$$

$$\sum_{h \in \mathcal{H}} \mathbf{Q} \cdot q_h(t_k) \leq \gamma \cdot \mathbf{D} \quad \forall k \in \mathcal{K}, \text{ and} \quad (8d)$$

$$q_h(t_k) \in \{0, 1\} \quad \forall k \in \mathcal{K}, h \in \mathcal{H}. \quad (8e)$$

In the next section, we present the receding-horizon algorithm to solve the above MILPs.

4.1. A Receding-Horizon (RH) algorithm

One issue that can hinder solving the MILPs to global optimality is the size of the MILPs. For the decentralized, look-ahead model, the reformulation produces one MILP for each house in $h \in \mathcal{H}$ that can be solved separately. From the two MILP constraint sets in Eq. (7) and (8), we see that the size of the MILPs can be very large when either Δt is small, or the optimization time horizon T is large, resulting in very large computation times to obtain global optimal solution. To address this issue, we use a Receding Horizon (RH) algorithm to solve problems with a large value of the optimization time horizon T . The approach involves breaking up the time horizon into smaller ones and solving the MILPs in each of these smaller time horizons sequentially. More formally, we split the time horizon $[0, T]$ into $[0, T_1], [T_1, T_2], \dots, [T_{m-1}, T_m]$ where $T_m = T$. We then solve m MILPs that correspond to each smaller time horizon sequentially. In doing so, the initial condition for the i^{th} MILP is obtained from the solution of the $(i-1)^{\text{th}}$ MILP's last time point. The schematic of the RH algorithm is shown in Fig. 3. We digress briefly to address a subtle point

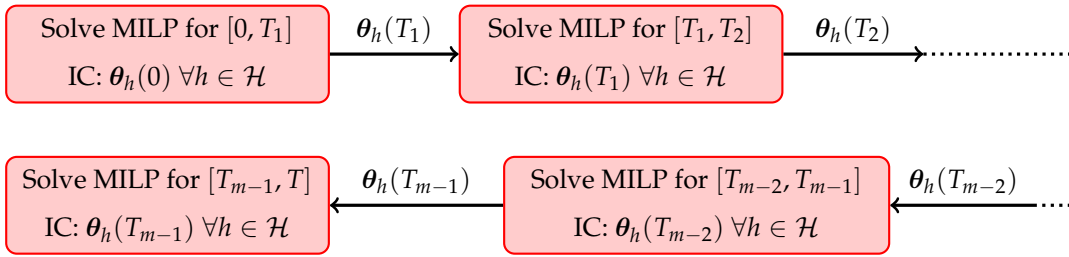


Figure 3: Schematic of the RH algorithm. IC denotes initial conditions.

regarding the discretization. The chosen value of Δt determines the granularity of the control q_h^g and as Δt becomes smaller, the approximation of the objective function also becomes more accurate. However, very fine grained control is practically useless; it would be pointless to toggle the state of the gas supply every minute for instance. Hence, we choose a time-spacing that is realistic with respect to the control variable. For our purposes, it is sufficient that the discretized equations are consistent with the ODE system they represent (as $\Delta t \rightarrow 0$, we recover the original system), and that is easily seen to be so.

4.2. Effects of coarser control discretization

From a practical standpoint, it is advantageous to choose a fine time-discretization for the state variables and a coarser time-discretization for the on-off control variable in each house. The motivation for using a coarser discretization for the control variables stems from the fact that gas-furnaces typically have a minimum on-time and off-time, i.e., if the furnace is switched on, it has to remain on for a certain time period and vice-versa. This feature of the gas furnace can be captured using a coarser discretization value (chosen using the minimum on- and off-times). Furthermore, doing so would also result in avoiding the effect of

chattering. In the next section, we present detailed case studies corroborating the effectiveness of all the formulations proposed in this article.

5. Case Studies

In this section, we present two case studies. The first case study analyses the efficacy of all the models presented in this article for a typical winter day in the Chicago area and the second case study analyses the impact of the 2019 Polar vortex in the Chicago area from the temperature data. For both the case studies, the set of houses and the parameters for each house remain unchanged. The Julia Programming language [40] was used for all the implementations and Gurobi [41] was used to solve the MILPs that were obtained by discretizing the OCPs. All the computational experiments were run on an Intel Broadwell E5-2695 processor with a base clock rate of 2.10 GHz and a RAM of 128 GB.

5.1. House data

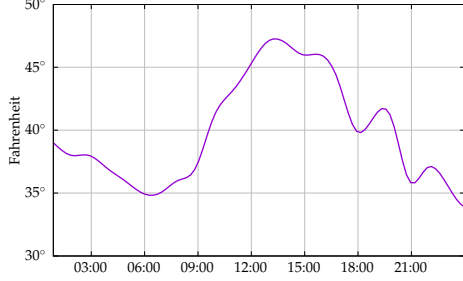
For all the case studies, the total number of houses in the set \mathcal{H} is set to 140. 14 categories of houses were chosen ranging from single bedroom apartments to single family homes. The thermal coefficients for each house was calculated according to the formulae derived in Appendix A. The furnace burn rate Q for each house was set in the range of $[3 \times 10^{-5}, 12 \times 10^{-5}] \text{ kg s}^{-1}$ depending on the square footage of the corresponding house. The value of the parameters specific to each house category like volume, square footage, initial temperature, set-point temperature etc. are made available at <https://github.com/kaarthiksundar/ng-dr-data>. The other parameter values used for computing the thermal coefficients for each house are shown in Table 1.

| Parameter | Value (SI Units) |
|--------------------------------------|--|
| C^a | $0.718 \times 10^3 \text{ (J kg}^{-1} \text{ K}^{-1})$ |
| ρ^a | $1.2754 \text{ (kg m}^{-3})$ |
| $\kappa_h \forall h \in \mathcal{H}$ | $0.11 \text{ (W m}^{-2} \text{ K}^{-1})$ |
| E^s | $45938 \times 10^3 \text{ (J kg}^{-1})$ |

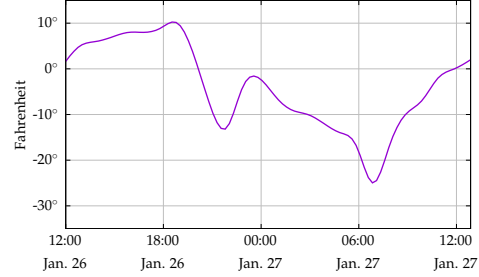
Table 1: Parameter values used for the case studies.

5.2. Ambient temperature data

For a typical winter day case study, the historical ambient temperature data for the Chicago area on January 2, 2020 was chosen. As for the polar vortex case, the temperature data from January 26, 2019 noon to January 27, 2019 noon was chosen. The temperature data for both cases were obtained from <https://www.noaa.gov/weather>. The plot of the temperature profiles for both the cases are shown in Figures 4a and 4b, respectively. Throughout the rest of the article, we shall refer to the two case studies by “typical-day” and “polar-vortex”.



(a) Ambient temperature data for the Chicago area on Jan. 2, 2020. This forecast is representative of a typical winter day in the Chicago area.



(b) Ambient temperature data for the Chicago area on Jan. 26-27, 2019. This is the day when the effect of the polar vortex was most severe.

Figure 4: Ambient temperature data for both the case studies in this article. Note that on the left, the temperature varies by at most 15 degrees, while on the right, the range is almost 40 degrees.

5.3. Results from the decentralized look-ahead model

Here we present the results obtained from the decentralized look-ahead model in Eq. (4) for both the case studies and compare it with the results from the baseline model in Eq. (1) and Eq. (2). For the decentralized look-ahead model, the value of λ_h for all the houses is varied in the set $\{0.65, 0.7, 0.75, 0.8, 0.85, 0.9, 0.95, 1\}$ and the look-ahead time period, denoted by T_{rh} (in hours) is chosen from the set $\{1, 3\}$. The look-ahead OCP for each house is solved separately but in parallel. Furthermore, the state and control discretization for the MILP reformulations for the look-ahead OCPs were set to 1 and 3 minutes, respectively.

| λ_h | Computation Time (seconds) | | Computation Time (seconds) | |
|-------------|----------------------------|-----------------|----------------------------|-----------------|
| | "typical-day" case | | "polar-vortex" case | |
| | $T_{rh} = 1$ hr | $T_{rh} = 3$ hr | $T_{rh} = 1$ hr | $T_{rh} = 3$ hr |
| 0.65 | 0.06 | 4.76 | 0.07 | 19.21 |
| 0.70 | 0.05 | 2.75 | 0.07 | 19.52 |
| 0.75 | 0.05 | 1.78 | 0.07 | 18.41 |
| 0.80 | 0.05 | 1.45 | 0.06 | 24.38 |
| 0.85 | 0.05 | 1.23 | 0.06 | 20.49 |
| 0.90 | 0.04 | 1.09 | 0.05 | 20.08 |
| 0.95 | 0.04 | 0.93 | 0.05 | 20.57 |
| 1.00 | 0.03 | 0.20 | 0.03 | 0.19 |

Table 2: Computation time in seconds for the decentralized look-ahead model averaged over all the houses. As T_{rh} increases, it is evident that the size of the MILP increases and hence, an increase in run time is observed for both the case studies as we move from $T_{rh} = 1$ hour to $T_{rh} = 3$ hours. In the text, we have explained why runs were not performed for a lower value of λ_h .

Table 2 shows the average computation time in seconds to solve the MILP corresponding to the decentralized look-ahead OCPs to optimality; the average is computed over all the houses since for each house

the decentralized model results in one MILP. As T_{rh} increases, it is evident that the size of the MILP increases and hence, an increase in run time is observed for both the case studies as we move from $T_{rh} = 1$ hour to $T_{rh} = 3$ hours. In the subsequent results, it will be made explicit as to why runs were not performed for a lower value of λ_h .

| model | λ_h | deviation ($^{\circ}$ F) | | | | gas consumption (kg) | consumption per house (kg) |
|---------------|-------------|---------------------------|-------|------|-----------|-------------------------|-------------------------------|
| | | mean | max. | min. | std. dev. | | |
| baseline | NA | 3.28 | 4.83 | 1.37 | 0.91 | 235.1538 | 1.6797 |
| decentralized | 0.65 | 7.71 | 36.99 | 1.38 | 10.92 | 155.5983 | 1.1114 |
| decentralized | 0.70 | 3.45 | 9.82 | 1.19 | 1.80 | 217.5768 | 1.5541 |
| decentralized | 0.75 | 2.74 | 3.60 | 1.19 | 0.65 | 225.3636 | 1.6097 |
| decentralized | 0.80 | 2.51 | 3.60 | 1.06 | 0.58 | 226.7347 | 1.6195 |
| decentralized | 0.85 | 2.38 | 3.40 | 1.06 | 0.55 | 227.2455 | 1.6232 |
| decentralized | 0.90 | 2.25 | 3.33 | 1.05 | 0.54 | 227.9151 | 1.6280 |
| decentralized | 0.95 | 2.17 | 3.33 | 1.05 | 0.54 | 228.2083 | 1.6301 |
| decentralized | 1.00 | 2.14 | 3.33 | 1.02 | 0.55 | 228.3865 | 1.6313 |

(a) "Typical-day" case study with $T_{rh} = 1$ hour

| model | λ_h | deviation ($^{\circ}$ F) | | | | gas consumption (kg) | consumption per house (kg) |
|---------------|-------------|---------------------------|------|------|-----------|-------------------------|-------------------------------|
| | | mean | max. | min. | std. dev. | | |
| baseline | NA | 3.28 | 4.83 | 1.37 | 0.91 | 235.1538 | 1.6797 |
| decentralized | 0.65 | 2.38 | 3.48 | 1.04 | 0.56 | 226.5980 | 1.6186 |
| decentralized | 0.70 | 2.31 | 3.48 | 1.04 | 0.55 | 227.2082 | 1.6229 |
| decentralized | 0.75 | 2.26 | 3.41 | 1.04 | 0.53 | 227.5393 | 1.6253 |
| decentralized | 0.80 | 2.21 | 3.33 | 1.04 | 0.54 | 227.8233 | 1.6273 |
| decentralized | 0.85 | 2.17 | 3.33 | 1.04 | 0.54 | 227.9923 | 1.6285 |
| decentralized | 0.90 | 2.15 | 3.33 | 1.04 | 0.55 | 228.2191 | 1.6301 |
| decentralized | 0.95 | 2.14 | 3.33 | 1.02 | 0.55 | 228.3163 | 1.6308 |
| decentralized | 1.00 | 2.14 | 3.33 | 1.02 | 0.55 | 228.3811 | 1.6313 |

(b) "Typical-day" case study with $T_{rh} = 3$ hour

Table 3: Statistics of temperature deviation and amount of gas consumed for the entire day for the "typical-day" case study. Note that reduction in gas consumption does not come at the cost of compromising on the deviation performance (in comparison to the baseline model). Thus, utilizing smart thermostats with look-ahead features can lead to substantial amount of reduction in consumption without compromising the deviation performance for a typical winter day.

The Tables 3 and 4 show the statistics of temperature deviation and the total gas consumption obtained

| model | λ_{ht} | deviation ($^{\circ}$ F) | | | | gas consumption (kg) | consumption per house (kg) |
|---------------|----------------|---------------------------|-------|------|-----------|-------------------------|-------------------------------|
| | | mean | max. | min. | std. dev. | | |
| baseline | NA | 5.97 | 14.70 | 2.41 | 3.70 | 560.9169 | 4.0065 |
| decentralized | 0.65 | 18.03 | 89.76 | 1.86 | 28.25 | 398.2451 | 2.8446 |
| decentralized | 0.70 | 7.03 | 20.21 | 1.74 | 4.88 | 545.9659 | 3.8998 |
| decentralized | 0.75 | 5.79 | 14.70 | 1.68 | 3.88 | 558.9702 | 3.9926 |
| decentralized | 0.80 | 5.53 | 14.70 | 1.63 | 3.99 | 562.1605 | 4.0154 |
| decentralized | 0.85 | 5.38 | 14.70 | 1.53 | 4.08 | 563.3577 | 4.0240 |
| decentralized | 0.90 | 5.30 | 14.70 | 1.53 | 4.14 | 563.9166 | 4.0280 |
| decentralized | 0.95 | 5.25 | 14.70 | 1.53 | 4.18 | 564.4836 | 4.0320 |
| decentralized | 1.00 | 5.23 | 14.70 | 1.53 | 4.19 | 566.9800 | 4.0499 |

(a) "Polar-vortex" case study with $T_{rh} = 1$ hour

| model | λ_{ht} | deviation ($^{\circ}$ F) | | | | gas consumption (kg) | consumption per house (kg) |
|---------------|----------------|---------------------------|-------|------|-----------|-------------------------|-------------------------------|
| | | mean | max. | min. | std. dev. | | |
| baseline | NA | 5.97 | 14.70 | 2.41 | 3.70 | 560.9169 | 4.0065 |
| decentralized | 0.65 | 5.51 | 14.82 | 1.60 | 4.18 | 559.5426 | 3.9967 |
| decentralized | 0.70 | 5.43 | 14.82 | 1.53 | 4.18 | 560.2889 | 4.0021 |
| decentralized | 0.75 | 5.36 | 14.75 | 1.53 | 4.20 | 560.9531 | 4.0068 |
| decentralized | 0.80 | 5.31 | 14.70 | 1.53 | 4.21 | 561.5633 | 4.0112 |
| decentralized | 0.85 | 5.25 | 14.70 | 1.53 | 4.18 | 562.8647 | 4.0205 |
| decentralized | 0.90 | 5.24 | 14.70 | 1.53 | 4.19 | 562.9878 | 4.0213 |
| decentralized | 0.95 | 5.23 | 14.70 | 1.53 | 4.19 | 563.2481 | 4.0232 |
| decentralized | 1.00 | 5.22 | 14.70 | 1.53 | 4.19 | 564.7536 | 4.0340 |

(b) "Polar-vortex" case study with $T_{rh} = 3$ hour

Table 4: Statistics of temperature deviation and amount gas of consumed for the entire day for the "polar-vortex" case study. We observe that though the reduction in gas consumption is not as substantial as in the "typical-day" case study, there exist regimes (λ_{ht} values) for which the decentralized look-ahead models provide minimal gas consumption reduction and good deviation performance.

using the decentralized look-ahead models for $T_{rh} \in \{1, 3\}$ hours. The deviation performance is a measure of discomfort caused to the households, i.e., greater the deviation numbers, the greater the discomfort. No runs were performed on the decentralized look-ahead model for values of $\lambda_{ht} < 0.65$ because, deviation performance was already unacceptable when $\lambda_{ht} = 0.65$. Decreasing the value of λ_{ht} any further would only decrease the natural gas consumption further at the expense of greater discomfort to the households.

In all the tables, the first row values are obtained by solving the baseline model. Furthermore, a lower value of the look-ahead time period results in more short-sightedness of the solutions; this is observed by the fact that reducing the value of T_{rh} decreases the deviation performance to achieve lower gas consumption. This trend can be observed in both the Tables 3 and 4. The case-study specific discussion of the results in Tables 3 and 4 is presented in the next paragraph.

For the “typical-day” case study results in Tables 3a and 3b, we observe substantial reduction in gas consumption per house for many values of λ_h . The values of the gas consumption per house indirectly show more aggregation benefits. For instance in Table 3a, when the value of $\lambda_h = 0.75$, the gas savings per house is 0.07 kg. When the number of houses aggregated is around 10000, this leads to a total gas consumption reduction of ≈ 700 kg, which in reality is a substantial amount of reduction in consumption even on a typical winter day. Furthermore, it is important to note that this reduction in gas consumption does not come at the cost of compromising on the deviation performance (in comparison to the baseline model). In summary, utilizing smart thermostats with look-ahead features can lead to substantial amount of reduction in consumption without compromising the deviation performance for a typical winter day. As for the “polar-vortex” case study, we observe that though the reduction in gas consumption is not as substantial as in the “typical-day” case study, there exist regimes (λ_h values) for which the decentralized look-ahead models provide minimal gas consumption reduction and good deviation performance. Also, unlike the “typical-day” case where one can always achieve consumption reduction for all λ_h values that provide deviation performance comparable to the baseline model, the values of λ_h closer to 1 cause an increase in the gas consumption. This is again expected due to the severity of the polar vortex. Nevertheless, if the operator can ensure all the smart thermostats for the decentralized model have the appropriate value of λ_h set, it can still lead to reduction in gas consumption. In the next section, we present results for the centralized look-ahead models.

5.4. Results from the centralized look-ahead models

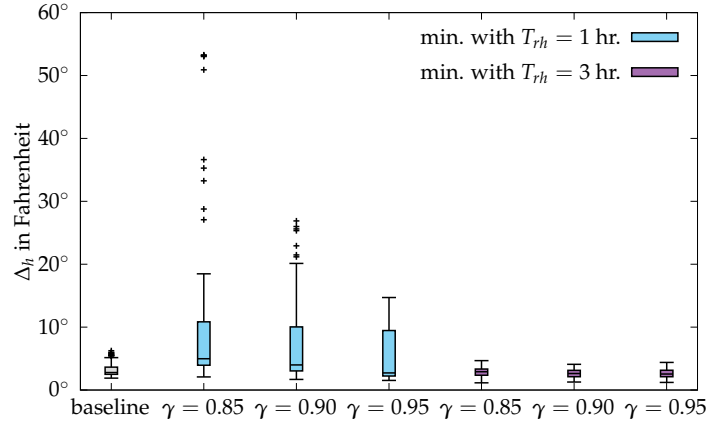
The centralized look-ahead model is more suited to perform what-if analysis on extreme event scenarios like the polar vortex or cold snaps. Hence, the following results are presented only for the “polar-vortex” case study. For a “typical-day” case study, the decentralized model is more suitable and provides the aggregation benefits that are detailed in Sec. 5.3. To that end, we choose the following parameters for the centralized model: (i) the value of D , the peak mass flow rate at any instant of time, is set to the maximum mass flow rate obtained by time integrating the baseline model for the “polar-vortex” case study and (ii) the value of the curtailment factor, γ , is chosen from the set $\{0.85, 0.90, 0.95\}$. Similar to the previous results, all the experiments for the centralized look-ahead models are run for $T_{rh} \in \{1, 3\}$ hours. In all the results presented hereafter, we shall use “min.” to denote the centralized look-ahead model with the mean deviation objective and “min. max.” to denote the max. deviation objective. Finally, a computation time limit of 1.5 hours was imposed on every run of the centralized look-ahead model.

| γ | Avg. computation time (sec) | | Avg. optimality gap (%) | |
|-----------------|-----------------------------|--------------|-------------------------|--------------|
| | $T_{rh} = 1$ | $T_{rh} = 3$ | $T_{rh} = 1$ | $T_{rh} = 3$ |
| min. model | | | | |
| 0.85 | TO | TO | 8.87 | 26.50 |
| 0.90 | TO | TO | 6.55 | 22.70 |
| 0.95 | TO | TO | 5.98 | 19.54 |
| min. max. model | | | | |
| 0.85 | 14.94 | 1590.21 | 0 | 0 |
| 0.90 | 14.19 | 948.91 | 0 | 0 |
| 0.95 | 13.31 | 766.85 | 0 | 0 |

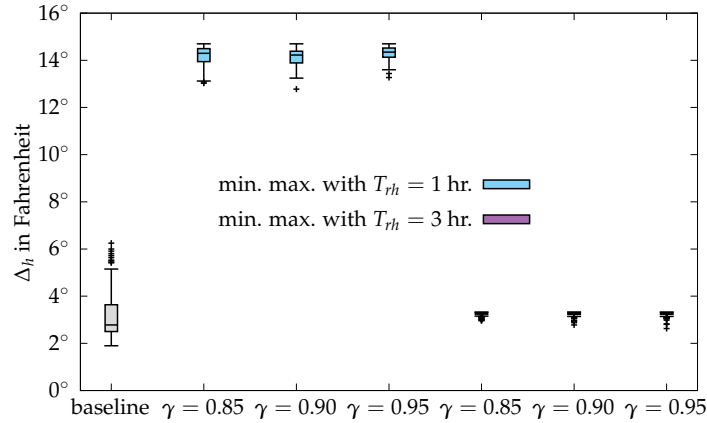
Table 5: Average computation times and optimality gaps for both the centralized look-ahead models. Here, “TO” implies all the runs for that particular value of look-ahead time period “timed-out”, i.e., did not complete within the allotted time limit of 1.5 hours. The high computation time and optimality gap values for the “min.” model when compared against the “min. max.” model can be explained by the fact the problem of minimizing the mean deviation for the centralized model can lead to a lot of degeneracy in the solution space of the OCPs. This degeneracy is removed when the objective is to minimize the maximum deviation and hence, the massive reduction in computation time. Also, when the value of T_{rh} increases, the number of variables and constraints in the centralized look-ahead model increases and this naturally increases the computation times.

Table 5 show the average computation time and the average optimality gap for all the runs of the centralized model with the two different objectives. In Table 5, the averages are computed over each run of the centralized MILP in Sec. 4.1. One immediate observation is the high computation time and optimality gap values for the “min.” model when compared against the “min. max.” model. This trend can be explained by the fact the problem of minimizing the mean deviation for the centralized model can lead to a lot of degeneracy in the solution space of the OCPs. This degeneracy is removed when the objective is to minimize the maximum deviation and hence, the massive reduction in computation time. Also, when the value of T_{rh} increases, the number of variables and constraints in the centralized look-ahead model increases and this naturally increases the computation times. Finally, as the value of γ decreases, the centralized models find a control policy with a bound on the natural gas consumption. In an extreme event setting, this can lead to finding optimal solutions more difficult; this in turn leads to increase in computational times. Physically, this is equivalent to constraining the capacity of the system. In the next set of results, we analyze the deviation performance of both the centralized models.

Consistent with results observed from the run-time and optimality gaps in Table 5, the box plots (Figure 5) also show that the “min.” model produces a deviation performance much worse than the “min. max.” model within computational time limit imposed. The spread of the data in Figure 5 reveals two salient trends: (i) When using the “min.” objective function, a 1 hour look-ahead leads to too big a spread in temperature deviation data. However, by using a 3 hour look-ahead, one can achieve peak reduction of



(a) Centralized look-ahead model with min. objective function.



(b) Centralized look-ahead model with min. max. objective function

Figure 5: Box plot of temperature deviation from the set point temperature for all the houses, i.e., Δ_h values for all the houses in the set \mathcal{H} . The spread of the data reveals two salient trends: (i) When using the “min.” objective function, a 1 hour look-ahead leads to too big a spread in temperature deviation data. However, by using a 3 hour look-ahead, one can achieve peak reduction of 5%, 10% or even 15% (corresponding to curtailment factor values of 0.95, 0.90, 0.85 respectively) with a deviation performance at least as good as the baseline model. (ii) When using the “min-max” objective function, a 1 hour look-ahead leads to unacceptably large temperature deviations even though the spread is limited. However, with a look-ahead of 3 hours, even 15% peak reduction is feasible with temperature deviation values and spread that are much lesser than the baseline.

5%, 10% or even 15% (corresponding to curtailment factor values of 0.95, 0.90, and 0.85, respectively) with a deviation performance at least as good as the baseline model. (ii) When using the “min-max” objective function, a 1 hour look-ahead leads to unacceptably large temperature deviations even though the spread is limited. However, with a look-ahead of 3 hours, even 15% peak reduction is feasible with temperature deviation values and spread that are much lesser than the baseline. This leads to a conclusion that if the technology and infrastructure is indeed set up for implementing the centralized models, it can provide the operator a more efficient way of providing equitable services to the customers without incurring a substantial increase in the natural gas consumption. Going further, the results from the centralized model allow one to conclude that equitable service can be provided while simultaneously reducing the peak natural gas consumption during an extreme event scenario.

In the next section, we present some future research directions given that this is the first work to develop optimization problem formulations for DR in a natural gas-only setting.

6. Future Research Directions and Conclusion

This study develops a series of models for natural gas demand response at the household level based on physics and thermodynamics, and demonstrates significant benefits of demand response in the field of natural gas. To demonstrate the feasibility of a demand response implementation for natural gas, we adopted simplified assumptions, such as considering only residential loads (home heating), assuming existence of smart thermostats, and ignoring pipeline network effects. Thus, residential loads (home heating) are treated as the sole consumers of natural gas. The natural gas pipeline network is ignored, and two kinds of smart thermostats are modelled. To make the study more realistic in the future, current research can be extended in the following directions: (i) inclusion of network effects due to the pipeline network and the study of its impact on the proposed DR models, (ii) formulation and solution of DR models that include uncertainty in the temperature forecast, (iii) data-driven estimation of the thermal coefficients of the house using measurements and the known uncertainty in the estimates of these coefficients, and finally (iv) quantify the link between time-based rate/economic incentives and direct load control.

In conclusion, our article represents the start of an interesting and important problem of designing demand response for a natural-gas only system. This work is timely given the realities of climate change; climate change is causing an increased number of severe winter weather events and this in turn is causing a stress on the natural gas pipeline networks, impeding the ability of these systems to provide equitable services to all its customers. The lack of resiliency of the natural-gas grid results in inconvenience, disruption and even loss of lives. The proposed DR models are a simple technique to increase the resiliency of the natural gas systems, leading to more efficient operation in severe events as well as normal winter weather. Nevertheless, large scale implementation of these models requires major technological and infrastructure investment as well as policy changes that need to be initiated by the federal government.

Declaration of Competing Interest

The authors declare that they have no competing interests.

Acknowledgement

This work was supported by the U.S. Department of Energy’s Advanced Grid Modeling (AGM) project *Joint Power System and Natural Gas Pipeline Optimal Expansion*. The research work conducted at Los Alamos National Laboratory is done under the auspices of the National Nuclear Security Administration of the U.S. Department of Energy under Contract No. 89233218CNA000001. We gratefully thank the AGM program manager Alireza Ghassemian for his support of this research.

Appendix A. Computation of thermal coefficients for a house

We consider a house $h \in \mathcal{H}$ and let θ_h^0 denote the initial temperature inside house h . We also let $\theta^o(t)$ be the given time-varying forecast of the ambient/outside temperature. Each house is assumed to have a gas furnace that burns fuel at the rate Q (kg s^{-1}). Also associated with each house h are the following constants: V_h - the volume of the house (m^3), κ_h - the heat transfer coefficient of the walls of the house based on insulation ($\text{W m}^{-2} \text{K}^{-1}$), A_h - the surface area of the walls of the house exposed to the outside temperature (m^2), $\bar{\theta}_h$ - the constant temperature set-point of the house (set by the occupants) (K). Finally, we let E^g (J kg^{-1}) be the specific heating value of natural gas. When the furnace is on, the heat flux produced by the furnace is given by $Q \cdot E^g$ (J s^{-1}).

Furthermore, the following statements are assumed about the physical system: the air inside the house undergoes an isochoric (constant volume) process, and hence the relevant specific heat of the gas C^a ($\text{J kg}^{-1} \text{K}^{-1}$) is the one calculated at constant volume. We assume that C^a is constant over the temperature range of interest. We also neglect the thermal compressibility (density dependence on temperature) of air and assume a constant density ρ^a (kg m^{-3}) over the temperature range of interest. The only source of heat supply is the furnace, and heat is constantly lost through the walls of the house at a rate proportional to the surface area of the walls and the difference in temperature between the house and the external environment.

Given these notations and assumptions, the dynamics of heat flow within the house h is governed by:

$$C^a \rho^a V_h \dot{\theta}_h(t) = -\kappa_h A_h (\theta_h(t) - \theta^o(t)) + Q \cdot E^g q_h^g(t). \quad (\text{A.1})$$

Comparing Eq. (A.1) and (1a), we can obtain expressions for the thermal coefficients α_h and β_h as:

$$\alpha_h = \frac{\kappa_h A_h}{C^a \rho^a V_h} \quad \text{and} \quad \beta_h = \frac{E^g}{C^a \rho^a V_h} \quad (\text{A.2})$$

In all the computational experiments, the thermal coefficients for each house is computed using Eq. (A.2).

References

- [1] Federal Energy Regulatory Commission, A national assessment of demand response potential, 2009.
- [2] F. E. R. Commission, National action plan on demand response, ????
- [3] M. T. Kelley, R. C. Pattison, R. Baldick, M. Baldea, An milp framework for optimizing demand response operation of air separation units, *Applied Energy* 222 (2018) 951–966. URL: <http://www.sciencedirect.com/science/article/pii/S0306261917318524>. doi:<https://doi.org/10.1016/j.apenergy.2017.12.127>.
- [4] E. P. R. Institute, The green grid: Energy savings and carbon emissions reductions enabled by a smart grid, 2008.
- [5] K. Borden, Amid an Extreme Heat Wave, PJM Turns to Demand Response to Maintain Grid Reliability, <https://energysmart.enelxnorthamerica.com/amid-extreme-heat-wave-pjm-turns-demand-response-maintain-grid-reliability>, 2019.
- [6] F. Shariatzadeh, P. Mandal, A. K. Srivastava, Demand response for sustainable energy systems: A review, application and implementation strategy, *Renewable and Sustainable Energy Reviews* 45 (2015) 343–350. URL: <http://www.sciencedirect.com/science/article/pii/S1364032115000726>. doi:<https://doi.org/10.1016/j.rser.2015.01.062>.
- [7] H. Goudarzi, S. Hatami, M. Pedram, Demand-side load scheduling incentivized by dynamic energy prices, in: 2011 IEEE International Conference on Smart Grid Communications (SmartGridComm), 2011, pp. 351–356.
- [8] A. Barbato, A. Capone, Optimization models and methods for demand-side management of residential users: A survey, *Energies* (2014) 5787–5824.
- [9] H. R. Massrur, T. Niknam, M. Fotuhi-Firuzabad, Investigation of carrier demand response uncertainty on energy flow of renewable-based integrated electricity–gas–heat systems, *IEEE Transactions on Industrial Informatics* 14 (2018) 5133–5142.
- [10] J. Wang, Y. Li, Y. Zhou, Interval number optimization for household load scheduling with uncertainty, *Energy and Buildings* 130 (2016) 613–624. URL: <http://www.sciencedirect.com/science/article/pii/S0378778816307903>. doi:<https://doi.org/10.1016/j.enbuild.2016.08.082>.
- [11] L. Bai, F. Li, H. Cui, T. Jiang, H. Sun, J. Zhu, Interval optimization based operating strategy for gas-electricity integrated energy systems considering demand response and wind uncertainty, *Applied Energy* 167 (2016) 270–279. URL: <http://www.sciencedirect.com/science/article/pii/S0306261915013550>. doi:<https://doi.org/10.1016/j.apenergy.2015.10.119>.

- [12] X. Zhang, M. Shahidehpour, A. Alabdulwahab, A. Abusorrah, Hourly electricity demand response in the stochastic day-ahead scheduling of coordinated electricity and natural gas networks, *IEEE Transactions on Power Systems* 31 (2016) 592–601.
- [13] Y. Zhang, Z. Huang, F. Zheng, R. Zhou, X. An, Y. Li, Interval optimization based coordination scheduling of gas–electricity coupled system considering wind power uncertainty, dynamic process of natural gas flow and demand response management, *Energy Reports* 6 (2020) 216–227. URL: <http://www.sciencedirect.com/science/article/pii/S2352484719311345>. doi:<https://doi.org/10.1016/j.egy.2019.12.013>.
- [14] C. He, X. Zhang, T. Liu, L. Wu, Distributionally robust scheduling of integrated gas–electricity systems with demand response, *IEEE Transactions on Power Systems* 34 (2019) 3791–3803.
- [15] L. Ju, R. Zhao, Q. Tan, Y. Lu, Q. Tan, W. Wang, A multi-objective robust scheduling model and solution algorithm for a novel virtual power plant connected with power-to-gas and gas storage tank considering uncertainty and demand response, *Applied Energy* 250 (2019) 1336–1355. URL: <http://www.sciencedirect.com/science/article/pii/S0306261919308803>. doi:<https://doi.org/10.1016/j.apenergy.2019.05.027>.
- [16] Y. Su, W. Nie, Y. Zhou, M. Tan, H. Qiao, An interval based cost-emissions optimization strategy for gas–electricity integrated energy systems under uncertainty and demand response, in: *2017 IEEE Conference on Energy Internet and Energy System Integration (EI2)*, 2017, pp. 1–6.
- [17] P. Bradley, M. Leach, J. Torriti, A review of the costs and benefits of demand response for electricity in the uk, *Energy Policy* 52 (2013) 312–327. URL: <http://www.sciencedirect.com/science/article/pii/S0301421512008142>. doi:<https://doi.org/10.1016/j.enpol.2012.09.039>, special Section: Transition Pathways to a Low Carbon Economy.
- [18] M. Qadrdan, M. Cheng, J. Wu, N. Jenkins, Benefits of demand-side response in combined gas and electricity networks, *Applied Energy* 192 (2017) 360–369. URL: <http://www.sciencedirect.com/science/article/pii/S0306261916314866>. doi:<https://doi.org/10.1016/j.apenergy.2016.10.047>.
- [19] A. Sheikhi, S. Bahrani, A. M. Ranjbar, An autonomous demand response program for electricity and natural gas networks in smart energy hubs, *Energy* 89 (2015) 490–499. URL: <http://www.sciencedirect.com/science/article/pii/S0360544215007318>. doi:<https://doi.org/10.1016/j.energy.2015.05.109>.
- [20] H. Cui, F. Li, Q. Hu, L. Bai, X. Fang, Day-ahead coordinated operation of utility-scale electricity and natural gas networks considering demand response based virtual power plants, *Applied Energy* 176

- (2016) 183–195. URL: <http://www.sciencedirect.com/science/article/pii/S030626191630589X>. doi:<https://doi.org/10.1016/j.apenergy.2016.05.007>.
- [21] L. Zhou, N. Liu, Y. Zhang, Energy management for smart energy hub considering gas dispatch factor and demand response, in: 2018 2nd IEEE Conference on Energy Internet and Energy System Integration (EI2), 2018, pp. 1–6.
- [22] F. Wang, H. Xu, T. Xu, K. Li, M. Shafie-khah, J. P. Catalão, The values of market-based demand response on improving power system reliability under extreme circumstances, *Applied Energy* 193 (2017) 220–231. URL: <http://www.sciencedirect.com/science/article/pii/S0306261917300971>. doi:<https://doi.org/10.1016/j.apenergy.2017.01.103>.
- [23] Y. Su, Y. Zhou, M. Tan, An interval optimization strategy of household multi-energy system considering tolerance degree and integrated demand response, *Applied Energy* 260 (2020) 114144. URL: <http://www.sciencedirect.com/science/article/pii/S0306261919318318>. doi:<https://doi.org/10.1016/j.apenergy.2019.114144>.
- [24] D. Wang, Q. Hu, H. Jia, K. Hou, W. Du, N. Chen, X. Wang, M. Fan, Integrated demand response in district electricity-heating network considering double auction retail energy market based on demand-side energy stations, *Applied Energy* 248 (2019) 656–678. URL: <http://www.sciencedirect.com/science/article/pii/S030626191930697X>. doi:<https://doi.org/10.1016/j.apenergy.2019.04.050>.
- [25] A. Halder, X. Geng, F. A. Fontes, P. Kumar, L. Xie, Optimal power consumption for demand response of thermostatically controlled loads, *Optimal Control Applications and Methods* 40 (2019) 68–84.
- [26] S. Bhattacharya, K. Kar, J. H. Chow, Optimal precooling of thermostatic loads under time-varying electricity prices, in: 2017 American Control Conference (ACC), IEEE, 2017, pp. 1407–1412.
- [27] S. Bhattacharya, K. Kar, J. H. Chow, Economic operation of thermostatic loads under time varying prices: An optimal control approach, *IEEE Transactions on Sustainable Energy* 10 (2018) 1960–1970.
- [28] M. Babula, K. Petak, The cold truth: Managing gas-electric integration: The iso new england experience, *IEEE power and energy magazine* 12 (2014) 20–28.
- [29] E. Cox, G. S. Schneider, Energy companies abandon long-delayed atlantic coast pipeline, *Washington Post* (July 5, 2020).
- [30] U. H. of Representatives, Energy and water development and related agencies for the fiscal year ending september 30, 2019, and for other purposes, 2019.

- [31] A. Balaskovitz, Polar vortex offers utility customers lesson in demand response, <https://energynews.us/2019/02/01/midwest/polar-vortex-offers-utility-customers-lesson-in-demand-response/>, 2013.
- [32] Y. Zhang, Y. He, C. Guo, M. Shahidehpour, C. Wang, Synergistic integrated electricity-natural gas system operation with demand response, 2018 IEEE Power & Energy Society General Meeting (PESGM) (2018) 1–5.
- [33] K. Tsai, U.s. natural gas consumption sets new record in 2019, <https://www.eia.gov/todayinenergy/detail.php?id=43035>, 2019.
- [34] M. M. Abahussain, R. D. Christie, Optimal scheduling of a natural gas processing facility with price-based demand response, in: 2013 IEEE Power Energy Society General Meeting, 2013, pp. 1–5.
- [35] M. Rudkevich, A. Zlotnik, Locational marginal pricing of naturalgas subject to engineering constraints, in: in Proc. 50th Hawaii Int. Conf.Syst. Sci., 2017, p. 3092–3101.
- [36] L. Lan, P. Wargocki, D. P. Wyon, Z. Lian, Effects of thermal discomfort in an office on perceived air quality, sbs symptoms, physiological responses, and human performance, *Indoor Air* 21 (2011) 376–390. URL: <https://onlinelibrary.wiley.com/doi/abs/10.1111/j.1600-0668.2011.00714.x>. doi:10.1111/j.1600-0668.2011.00714.x. arXiv:<https://onlinelibrary.wiley.com/doi/pdf/10.1111/j.1600-0668.2011.00714.x>.
- [37] R. Jevons, C. Carmichael, A. Crossley, A. Bone, Minimum indoor temperature threshold recommendations for english homes in winter – a systematic review, *Public Health* 136 (2016) 4–12. URL: <http://www.sciencedirect.com/science/article/pii/S0033350616000640>. doi:<https://doi.org/10.1016/j.puhe.2016.02.007>.
- [38] L. Lan, P. Wargocki, Z. Lian, Quantitative measurement of productivity loss due to thermal discomfort, *Energy and Buildings* 43 (2011) 1057–1062. URL: <http://www.sciencedirect.com/science/article/pii/S0378778810003117>. doi:<https://doi.org/10.1016/j.enbuild.2010.09.001>, tackling building energy consumption challenges - Special Issue of ISHVAC 2009, Nanjing, China.
- [39] J.-J. E. Slotine, W. Li, *Applied Nonlinear Control*, Prentice hall Englewood Cliffs, NJ, 1991.
- [40] J. Bezanson, A. Edelman, S. Karpinski, V. B. Shah, *Julia: A fresh approach to numerical computing*, *SIAM review* 59 (2017) 65–98.
- [41] B. Bixby, *The Gurobi optimizer*, *Transporation Research Part B* 41 (2007) 159–178.